Review

# Fundamental Heating Characteristics of an RF Hyperthermic System Using a Rectangular Resonant Cavity Applicator for Deep-Seated Tumors

YUTAKA TANGE[1]*, YOSHIAKI SAITOH[2], YASUSHI KANAI[3], JUNICHI HORI[2]

[1]Graduate School of Science and Technology, Niigata University, 8050 Ikarashi 2-no-cho, Niigata 950-2181, Japan.
[2]Department of Biocybernetics, Faculty of Engineering, Niigata University, 8050 Ikarashi 2-no-cho, Niigata 950-2181, Japan.
[3]Department of Information and Electronics Engineering, Niigata Institute of Technology, 1719 Fujihashi, Kashiwazaki 945-1195, Japan.

Abstract: Many heat applicators for hyperthermia have been developed; however, in treatment of noninvasive cancer they can heat only the body surface. At present, it is difficult to selectively heat deep-seated tumors.

It is desirable to develop an applicator with the potential for heating a limited region, but achieving this objective is impossible with present technology. Therefore, our goal is to develop an applicator that can uniformly heat to deep regions of the human body.

In this paper, we describe fundamental heating characteristics of an RF hyperthermic system using a rectangular resonant cavity applicator for deep-seated tumors. First, electromagnetic and heat-transfer equations were solved to investigate fundamental heating characteristics of the resonant cavity applicator. In the experiments, a torso-shaped dielectric phantom, which has electrical constants close to human muscle, was used. In comparisons of the measured and calculated results, the tendencies of both heat distributions were in accordance. These results indicated the possibility of heating deep regions; thus, this applicator has the potential to heat deep-seated tumors.

Key Words: deep-seated tumors, human muscle constants, hyperthermia, numerical simulations, rectangular resonant cavity applicators

## Introduction

World Health Organization (WHO) statistics show that six million people worldwide die of cancer and that ten million new patients are added every year[1)].

Hyperthermia is a cancer treatment that focuses on differences in heat sensitivity between normal

Received 1 September 2005, Accepted 19 December 2005.*Corresponding author, Tel: +81-25-262-7435; Fax: +81-25-264-2024; E-mail: tange@mbe.bc.niigata-u.ac.jp

cells (alive until 44°C) and cancer cells (dead above 42.5°C)[2]. The treatment exposes cancer cells to high temperatures and kills them by utilizing, for example, electromagnetic waves. Compared to surgery, radiation therapy, and anticancer drug therapy, hyperthermia is an important method because of the possibility of reducing a patient's pain and suffering.

Many heat applicators for hyperthermia have already been developed. For example, radio frequency (RF) heat[3] and microwave heat[4] applicators are currently utilized in medicine. However, applicators in noninvasive cancer treatments heat only the body surface. Annular phased array (APA) systems, using the principle of phased arrays[5][6], can heat deep-seated tumors selectively. However, it is difficult to control the phases and amplitudes of multiple antennas to focus electromagnetic energy[7][8].

We have already developed a reentrant resonant cavity applicator targeting deep-seated tumors[9-12]. This applicator, as seen from the outside, is suitable to heat a disk-shaped dielectric phantom, and an object having a small diameter, such as the size of a human head, can be selectively heated to the deep region. However, it was impossible to heat an object within the human abdomen. Therefore, we developed an RF rectangular resonant cavity applicator using a torso-shaped dielectric phantom similar to the human abdomen[13][14]. Our studies showed that this applicator had the ability to heat deep regions if the antenna's shape and location were changed[15][16].

In this paper, we report on fundamental heating characteristics of an RF hyperthermic system using a rectangular resonant cavity applicator for deep-seated tumors. First, electromagnetic and heat-transfer equations were solved to investigate fundamental heating characteristics of the resonant cavity applicator. In the experiments, we introduced a torso-shaped dielectric phantom with electrical constants close to those of human muscle. We had originally placed an L-type antenna in a vertical position next to the dielectric phantom to achieve deep heating. However, this time the L-type antenna was placed in a horizontal position along the dielectric phantom. We obtained better deep heating results with this position than with the vertical position used in previous studies.

## Materials and Methods

### *Dielectric phantom*

According to the Federal Communications Commission web site[17], electrical conductivity and permittivity of a real human muscle in a frequency range of 60 MHz are $\sigma=0.7$ (S/m) and $\varepsilon_r=70$, respectively. Therefore, we introduced the torso-shaped dielectric phantom ($\phi$300 mm x 1100 mm) with electrical constants close to the real human muscle at approximately 20°C. We kept both the room temperature and the dielectric phantom's temperature at approximately 20°C for more than 12 hours by using an air conditioner. The materials of the dielectric phantom, TX-151 powder (12.8%), water (85.7%), and agar powder (1.5%), were uniformly mixed. The temperature and frequency dependences of the electrical constants were measured by our measurement system using an open-ended coaxial probe[18] prior to the calculation, as shown in Fig. 1.

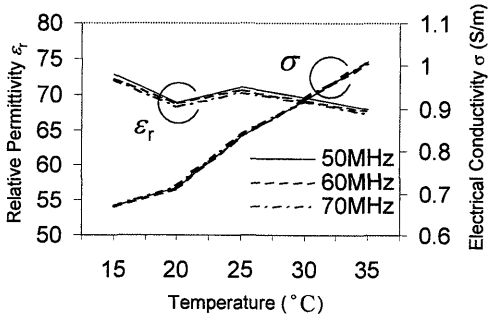


**Fig. 1.** Electrical constants of a torso-shaped dielectric phantom.

### *Principle of deep heating*

The resonant cavity applicator with the dielectric phantom was designed to produce a standing wave when electromagnetic fields in the resonant cavity applicator are generated by an L-type antenna. Therefore, high frequency current is induced in the dielectric phantom, which heats the deep region by passing current through it. This is called Joule heating.

### *Hyperthermic system using an RF rectangular resonant cavity applicator*

The experimental setup used in this study is shown in Fig. 2. Our hyperthermic system consists of a signal generator (G1057VG ; Tokyo HY-Power Labs., Inc.), a set of high frequency electric power amplifiers (PA2000J ; Niigata Tsushinki Co., Ltd.), two power meters (Model 43 ; BIRD Electronic Corp.), two custom impedance matching boxes, an L-type antenna, and a resonant cavity applicator.

The structure of the resonant cavity applicator is shown in Fig. 3. The resonant cavity applicator is made of 0.5 mm thick copper and the dimensions are 1300 mm x 1450 mm x 1500 mm. The wooden table is composed of a top plate with dimensions of 1200 mm x 35 mm x 400 mm and four legs $\phi$70 mm x 555 mm in size. Figure 4 depicts the structure of the L-type antenna system. We used a cylindrical copper bar ($\phi$6 mm ; Mitsubishi Materials Corp.) to make the antenna. The vertical L-type antenna was placed in the position where x=0 mm, −225 mm, and −450 mm, respectively. We found that better heating patterns are obtained by moving the antenna away from the applicator's center[14-16]. Therefore, a horizontal L-type antenna was placed in the position where x=−450 mm (Fig. 5 (b)).

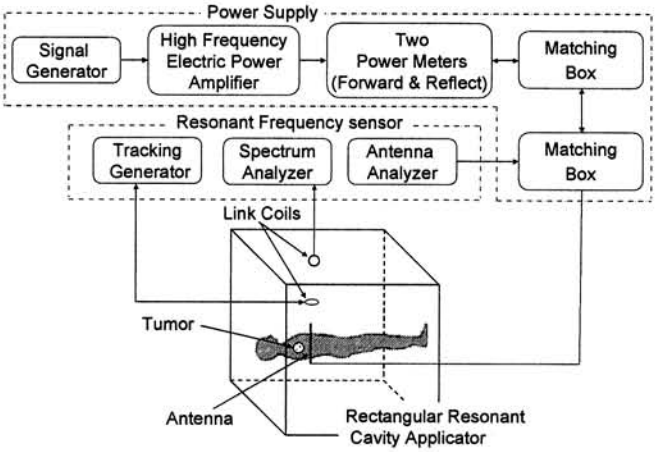


**Fig. 2.** Schematic of our experimental setup.

### *Numerical Methods*

Figure 6 shows flow diagrams for electromagnetic and heat-transfer analysis. Figure 7(a) shows a model for electromagnetic analysis. The model consists of a wooden table, L-type

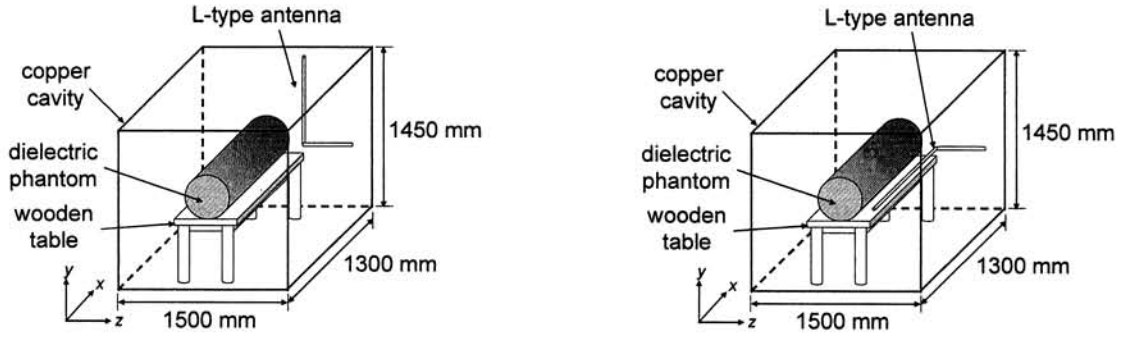


(a) Vertical L-type antenna system

(b) Horizontal L-type antenna system

**Fig. 3.** Arrangement of a rectangular resonant cavity applicator.

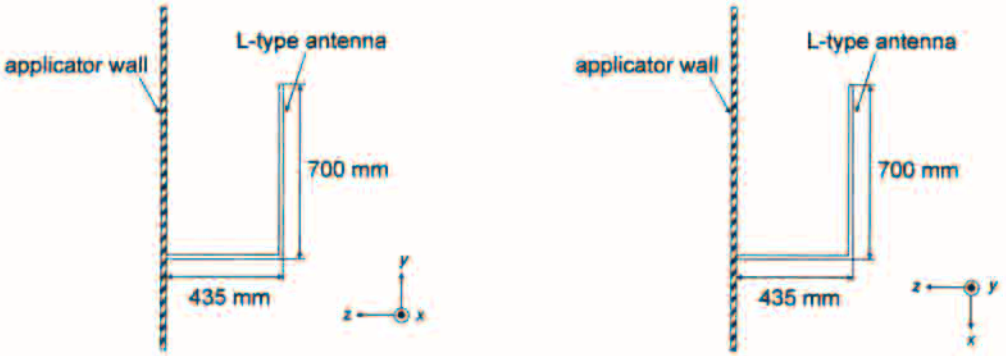


(a) Vertical L-type antenna system　　(b) Horizontal L-type antenna system

**Fig. 4.** Structure and setup of the L-type antenna.

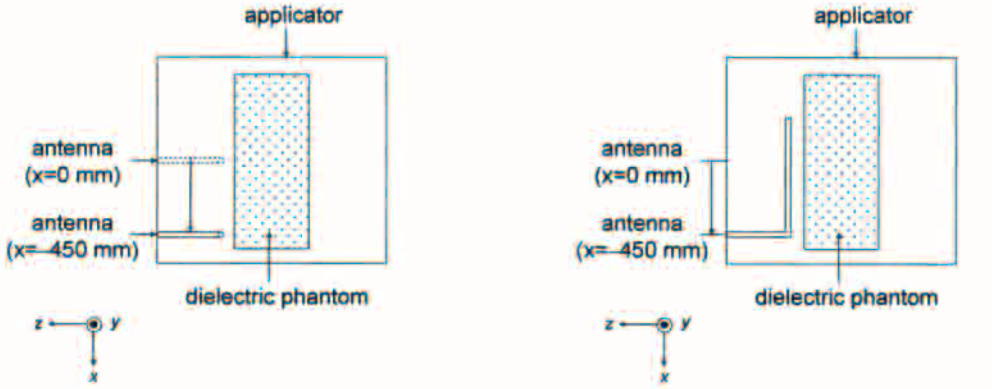


(a) Vertical L-type antenna system　　(b) Horizontal L-type antenna system

**Fig. 5.** Location of the L-type antenna (x = −450 mm).

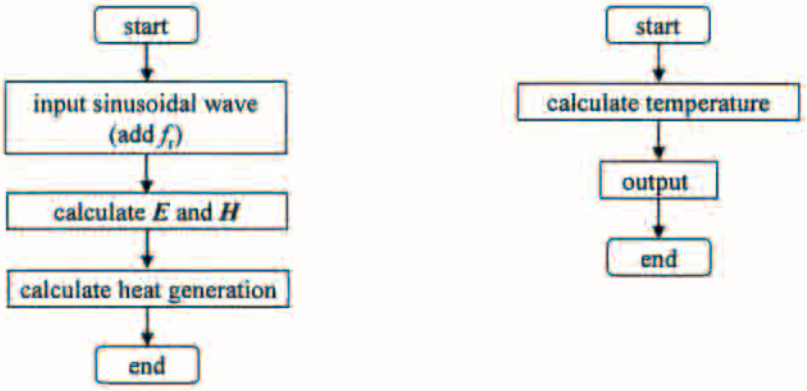


(a) Electromagnetic analysis　　(b) Heat-transfer analysis

**Fig. 6.** Flow diagrams for electromagnetic and heat-transfer analysis.

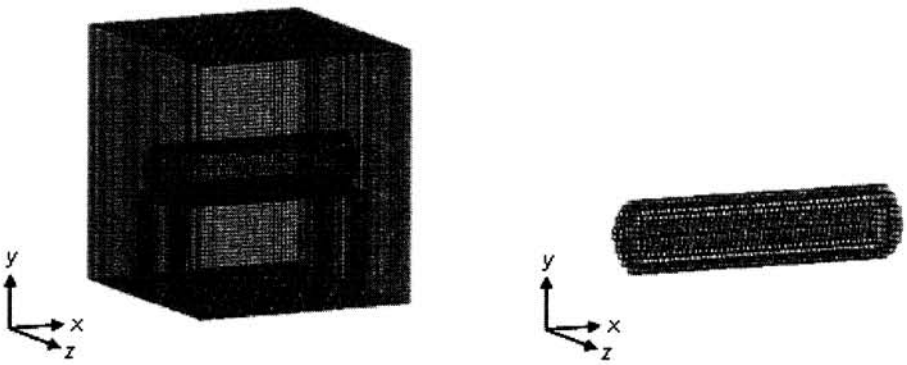


(a) Electromagnetic analysis (b) Heat-transfer analysis

**Fig. 7.** Analytical models for electromagnetic and heat-transfer analysis.

antenna, dielectric phantom, and resonant cavity applicator. Figure 7(b) shows a model for heat-transfer analysis. We considered only the phantom because the wooden table does not affect heat transfer in the dielectric phantom. These models were composed of regular mesh with sides of 25 mm and 12.5 mm respectively, using our mesh generator[19]. The cavity walls were assumed to be the loss-less walls.

We have applied three dimensional finite-difference time-domain methods[20] to solve Maxwell's equations :

$$\nabla \times \mathbf{E} = -\mu \frac{\partial \mathbf{H}}{\partial t}, \tag{1}$$

$$\nabla \times \mathbf{H} = \sigma \mathbf{E} + \varepsilon \frac{\partial \mathbf{E}}{\partial t}. \tag{2}$$

where, $\mu$, $\sigma$, and $\varepsilon$ represent permeability, electrical conductivity, and permittivity, respectively. The L-type antenna was modeled by using thin wire approximation[21] applied voltage source. The resonant frequency was derived from the electromagnetic analysis, and the lowest resonant frequency $f_r$ was applied. Electromagnetic energy was estimated as

$$\dot{Q} = \frac{1}{T} \sigma \int |\mathbf{E}|^2 dt. \tag{3}$$

Heat-transfer equations

$$\rho c \frac{\partial T}{\partial t} = \lambda \nabla^2 T + \dot{Q}, \tag{4}$$

$$q = \alpha_c (T - T_c), \tag{5}$$

have applied three dimensional finite element methods. $\rho$, c, $\lambda$, q, $\alpha_c$, and $T_c$ denote the volume density of mass, specific heat capacity, thermal conductivity, heat flux, heat transfer coefficient, and the external temperature, respectively. The thermal constants of the dielectric phantom were assumed to be $\rho = 1030$ (kg/m$^3$), c$=3150$ (J/kg•°C), $\lambda = 0.555$ (W/m•°C), and $\alpha_c = 5$ (W/m$^2$•°C)[10]. The electrical constants of the wooden table were assumed to be $\sigma = 0.0003$ (S/m) and $\varepsilon_r = 1.88$[22].

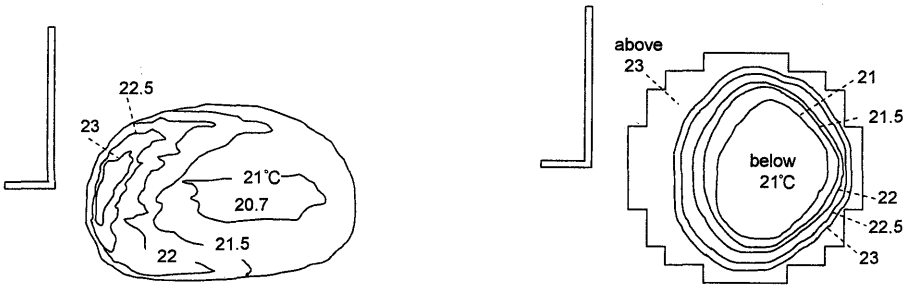


(a) measured result ($f_r$=61.62 MHz)　　(b) calculated result ($f_r$=61.69 MHz)

**Fig. 8.** Vertical L-type antenna (solid line) was placed at x=0 mm. Measured and calculated temperature distributions on the cross section at x=0 mm, where, $T_0$ and $T_c$ were 20.5°C and 20.8°C, respectively.

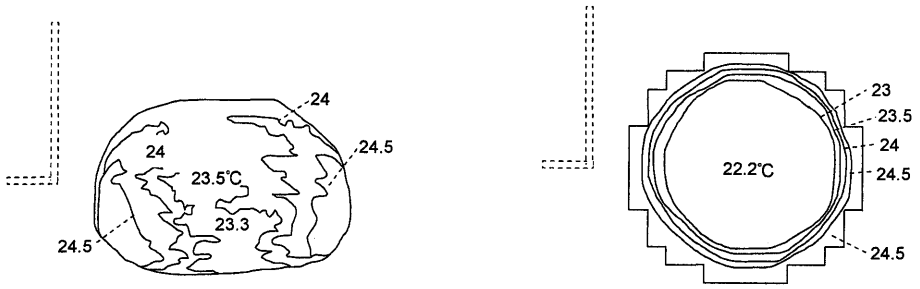


(a) measured result ($f_r$=62.23−62.27 MHz)　　(b) calculated result ($f_r$=63.48 MHz).

**Fig. 9.** Vertical L-type antenna (dotted line) was placed at x=−450 mm. Measured and calculated temperature distributions on the cross section at x=0 mm, where, $T_0$ and $T_c$ were 21.4°C and 21.5°C, respectively.

### *Experiments*

Electromagnetic power of 400 watts amplified by the amplifier in the frequency range from 60 to 65 MHz was applied to the antenna set inside the cavity applicator. The exciting frequency was defined as the resonant frequency and was derived from calculated results in advance. We confirmed this resonant frequency using a spectrum analyzer (Spectrum Analyzer MS2601A ; Anritsu Corp.). During the experiment, the dielectric phantom expands because of the temperature dependence of the materials. The matching box was adjusted because the reflected power increases by the change of capacitance between the antenna and the dielectric phantom. After the experiment, which lasted 30 minutes, the dielectric phantom was divided into cross sections and heat distributions were observed by thermography (Infra-Eye210 ; Fujitsu Co., Ltd.).

## Results and Discussion

### *a) Validity of our calculation*

In electromagnetic analysis using finite-difference time-domain methods, it is said that the stability condition[23] is as follows.

$$\text{mesh size} \leq \lambda_{\text{wavelength}} / 10, \tag{6}$$

where $\lambda_{wavelength}$ is the wavelength inside the dielectric phantom. A mesh size of 25 mm in our calculation is sufficient to satisfy this condition because the value of the stability condition in this case is 60 mm.

***b) Comparison of measured and calculated results***

Measured and calculated results obtained in this study are shown in Figs. 8-10, where the vertical antenna was set at x=0 in Fig. 8 and at x=−450 mm in Fig. 9, and the horizontal antenna was placed at x=−450 mm in Fig. 10.

The starting temperature $T_0$, room temperature $T_c$, and resonant frequency $f_r$, for each condition are listed in the figure captions. The shape of the measured results differs from the calculated ones because the experimental dielectric phantom is a gel. The calculated results, as shown in Figs. 8-10, cannot be compared with each other directly because of the introduction of constants into the heat-transfer analysis. The constants were decided on as approximately corresponding to the measured results. The tendencies of heat distributions of the measured and calculated results in Figs. 8-10 are in accord. Resonant frequencies of the measured and calculated results also are in accord.

The measured result (Fig. 8) demonstrates that the focus of the heated region is on the surface of the dielectric phantom. As shown in Fig. 9, the measured result shows that the concentration of the heated region was not only on the surface, but in the deep region, and that the temperature of the deep region rose. In this case, the vertical L-type antenna was set at x=−450 mm. The increases in temperature of the deep region from the original state in Figs. 8 and 9 were 0.2°C and 1.9°C, respectively. It is very important to move the vertical L-type antenna away from the applicator's center to achieve heating of the deep region. Perhaps the vertical L-type antenna can possibly disturb the electromagnetic fields in the resonant cavity applicator when the antenna is placed at the center (x=0 mm).

Measured and calculated results for the cross section (Fig. 10) show that the surface of the dielectric phantom was heated. In addition, the heated region of the dielectric phantom spread from the left to the right side of the deep region. The increase in temperature of the deep region from the original state in Fig. 10 was 2.1°C. In comparing the temperature increase between Figs. 9 and 10, Fig. 10 shows a slightly higher temperature 0.2°C. We believe that our applicator can be used to treat deep-seated tumors of the human abdomen. While the temperature difference is slight at present, we feel that higher temperatures can be achieved if electromagnetic power could rise above 400 watts and heating duration could be prolonged in clinical applications.

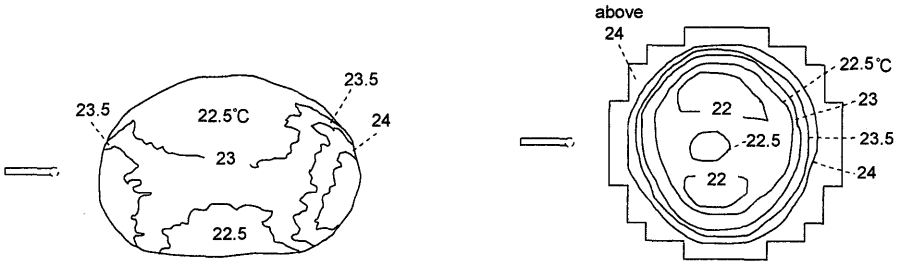


(a) measured result ($f_r$=62.02 MHz)

(b) calculated result ($f_r$=62.74 MHz)

**Fig. 10.** Horizontal L-type antenna (dotted line) was placed at x=−450 mm. Measured and calculated temperature distributions on the cross section at x=0 mm, where, $T_0$ and $T_c$ were 20.3°C and 20.7°C, respectively.

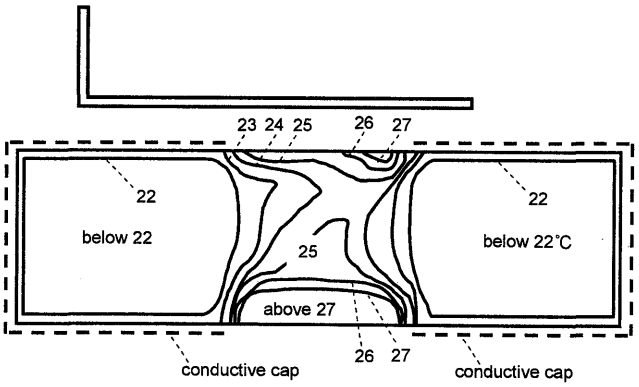


**Fig. 11.** Example for the calculated result of the dielectric phantom with conductive caps. Result shows heating distribution for the central horizontal plane of the dielectric phantom.

The measured and calculated results shown here are only for the cross section at x=0 mm, and note that the other cross sections as well as the central cross section (x=0 mm) were also heated. If conductive caps are attached to the dielectric phantom, sections can be protected by shielding the electromagnetic fields. Fig. 11 shows an example of the calculated result.

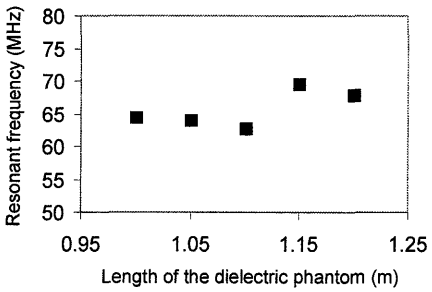


**Fig. 12.** Relationship of resonant frequency and length of the dielectric phantom, where the diameter is $\phi$300 mm.

The analytical condition in Fig. 12 is similar to that in Fig. 10. From the results in Fig. 12, the resonant frequency moves when the length of the dielectric phantom is changed. Instances when conductive caps and a bolus were attached to the dielectric phantom were also analyzed. The resonant frequencies of the dielectric phantom attached to conductive caps with a size of $\phi$300 mm (diameter) x 400 mm (width) and a bolus of $\phi$350 mm (diameter) x 300 mm (width) x 25 mm (thickness) were 63.18 MHz and 62.87 MHz, respectively. These results provide evidence that the resonant frequencies vary according to the dielectric phantom. It is easy to predict the resonant frequency by numerical analysis. Heating experiments should be performed after confirmation of the resonant frequency by using a spectrum analyzer.

In the future, we have plans to obtain better heating patterns than shown in this study by changing the antenna's shape and location. Also, we think that human blood flow must be considered in the calculations and experiments to elucidate thermal transfer characteristics of the human body.

## Acknowledgments

The authors would like to acknowledge the advice of Prof. Michio Miyakawa (Niigata University) for the measurements of phantom constants, and Messrs. Hiroki Ishiwatari, Tsuyoshi Satoh, and Kentarou Sunaga of our laboratory in Niigata University for their experimental and related assistance.

## References


1) World Health Organization web site [Online]. Available: (http://www.who.int/cancer/en/).
2) Dewey W. C., Hopwood L. E.: Cellular responses to combinations of hyperthermia and radiation. Radiology, 123: 463-474, 1977.
3) Takahashi H., Tanaka R., Watanabe M., Kakinuma K., Suda T., Takahashi S., Masuda H., Saito A., and Nakajima T.: Clinical results of RF interstitial hyperthermia for malignant brain tumors, Jpn J Hyperthermic Oncology, 11: 61-67, 1995. (Japanese).
4) Durney C. H.,Christensen D. A.: Introduction to Bioelectromagnetics, Boca Raton: CRC, 151-153, 1999.
5) Turner P. F.: Regional hyperthermia with an annular phased array, IEEE Trans. on Biomed. Eng., 31: 106-114, 1984.
6) Terada N., Amemiya Y.: The performance of the dipole array applicator for radiofrequency hyperthermia, The IEICE Transactions on Communications, J67-B: 163-170, 1984. (Japanese).
7) Siauve N., Nicolas L., Vollaire C., Nicolas A., and Vasconcelos J. A.: Optimization of 3-D SAR distribution in local RF hyperthermia, IEEE Trans. on Magn., 40: 1264-1267, 2004.
8) Wust P., Hildebrandt B., Sreenivasa G., Rau B., Gellermann J., Riess H., Felix R., and Schlag P. M.: Hyperthermia in combined treatment of cancer, The LANCET Oncology, 3: 487-497, 2002.
9) Kato K., Matsuda J., and Saitoh Y.: A re-entrant type resonant cavity applicator for deep-seated hyperthermia treatment, Proc. Annual Int'l Conf. of the IEEE Eng. in Medicine and Biology Society, 11: 1712-1713, 1989.
10) Kanai Y., Tsukamoto T., Toyama K., Saitoh Y., Miyakawa M., and Kashiwa T.: Analysis of a hyperthermic treatment in a reentrant resonant cavity applicator by solving time-dependent electromagnetic-heat transfer equations, IEEE Trans. on Magn., 32: 1661-1664, 1996.
11) Kanai Y., Tsukamoto T., Saitoh Y., Miyakawa M., and Kashiwa T.: Analysis of a hyperthermic treatment using a reentrant resonant cavity applicator for a heterogeneous model with blood flow, IEEE Trans. on Magn., 33: 2175-2178, 1997.
12) Yabuhara T., Kato K., Tsuchiya K., Shigihara T., Kohara T., Uzuka T., Takahashi H. and Tanaka R.: Improvement of the resonant cavity applicator for brain tumor hyperthermia -experimental heating results-, Proc. Annual Int'l Conf. of the IEEE Eng. In Medicine and Biology Society, 271, 2005.
13) Soeta S., Yokoo S., Shimada M., Kanai Y., and Hori J.: Eigenmode analysis of a parallelepiped resonator for hyperthermic treatment by using FD-TD method, 10th Niigata Branch Regional Meeting of IEE Japan, III-21, 2001. (Japanese).
14) Tange Y., Kanai Y., and Saitoh Y.: Analysis and development of a radio frequency rectangular resonant cavity applicator with multiple antennas for a hyperthermic treatment, IEEE Trans. on Magn., 41: 1880-1883, 2005.
15) Tange Y., Kanai Y., Saitoh Y., and Kashiwa T.: New heating characteristics of a radio frequency rectangular resonant cavity applicator using dipole antennas for hyperthermic treatment, The 15th Conference on the Computation of Electromagnetic Fields (IEEE COMPUMAG 2005), 2: 206, 2005.
16) Tange Y., Kanai Y., and Saitoh Y.: Heating characteristics of an RF hyperthermia for deep-seated region, Proc. Annual Int'l Conf. of the IEEE Eng. In Medicine and Biology Society, 271, 2005.
17) Federal Communications Commission web site [Online]. Available: (http://www.fcc.gov/fcc-bin/dielec.sh/).
18) Hoshina S., Kanai Y., and Miyakawa M.: A numerical study on the measurement region of an open-ended coaxial probe used for complex permittivity measurement, IEEE Trans. on Magn., 37: 3311-3314, 2001.
19) Kanai Y., Sato K.: Automatic mesh generation for 3D electromagnetic field analysis by FD-TD method, IEEE Trans. on Magn., 34: 3383-3386, 1998.
20) Sullivan D.: Three-dimensional computer simulation in deep regional hyperthermia using the finite-difference time-domain method, IEEE Trans. on Microwave Theory Tech., 38: 204-211, 1990.

21) Umashankar K. R., Taflove A., and Beker B.: Calculation and experimental validation of induced currents on coupled wires in an arbitrary shaped cavity, IEEE Trans. on Antennas Propagat., 35: 1248-1257, 1987.
22) Von Hippel A. R.: Dielectric Material and Applications, 3rd ed., Boston: The M.I.T. Press, 359, 1961.
23) Uno T.: Finite difference time domain method for electromagnetic field and antennas, Tokyo: Corona Publishing, 50-55, 2000.

# 立体空洞共振器を用いた深部癌温熱治療用RFシステムの基礎的な加温特性

丹下　裕[1]・斉藤義明[2]・金井　靖[3]・堀　潤一[2]

[1]新潟大学大学院・自然科学研究科
[2]新潟大学・工学部・福祉人間工学科
[3]新潟工科大学・情報電子工学科

**要　　旨**：多くの癌温熱治療用加温装置が開発されている．しかしながら．非侵襲な癌温熱治療用加温装置は，人体表面近傍のみの加温が可能である．現状では，RF波を用いて深部に位置する癌を選択的に加温することは不可能である．

局部加温の可能性を持つ装置を開発することが望ましいが，この目標を達成することは，現状の技術では不可能である．それゆえ，我々は，人体深部までを一様に加温する装置を開発することを目標とした．

この論文では，立体空洞共振器を用いた深部癌温熱治療用RFシステムの基礎的な加温特性について述べる．初めに，基本加温特性を調べるためにMaxwellの方程式と熱伝導—熱伝達方程式を解いた．次に，人体筋肉の電気特性を模した誘電体ファントムを使用し，加温実験を行った．実験結果と計算結果を比較したところ，深部加温できる傾向は一致した．すなわち，深部癌温熱治療用加温装置としての可能性を持つことが分かった．